Pharmaceutical Research, Vol. 23, No. 1, January 2006 (© 2006)
DOI: 10.1007/s11095-005-8814-3

Research Paper

Pharmacokinetics/Pharmacodynamics of Nondepleting Anti-CD4 Monoclonal Antibody (TRX1) in Healthy Human Volunteers

Chee M. Ng,[1,3] Eric Stefanich,[1] Banmeet S. Anand,[1] Paul J. Fielder,[1] and Louis Vaickus[2]

Received July 29, 2005; accepted September 28, 2005

Purpose. TRX1 is a nondepleting anti-CD4 monoclonal IgG1 antibody being developed to induce tolerance by blocking CD4-mediated functions. The purpose of this study is to describe the pharmacokinetics (PK) and pharmacodynamics (PD) of TRX1 and to develop a receptor-mediated PK/PD model that characterizes the relationships between serum TRX1 concentration and total and free CD4 expression in healthy male volunteers.
Methods. Nine subjects from three dosing cohorts in double-blinded, placebo-controlled phase I clinical study was included in the analysis. Serum TRX1 levels were determined using enzyme-linked immunosorbent assay. Blood total and free CD4 receptor levels were determined by using flow cytometric analyses. The receptor-mediated PK/PD model was developed to describe the dynamic interaction of TRX1 binding with CD4 receptors.
Results and Conclusions. TRX1 displayed nonlinear pharmacokinetic behavior and the CD4 receptors on T cells were saturated and down-modulated following treatment with TRX1. Results from *in vitro* studies using purified human T cells suggested that CD4-mediated internalization may constitute one pathway by which CD4 is down-modulated and TRX1 is cleared *in vivo*. The developed receptor-mediated PK/PD model adequately described the data. This PK/PD model was used to simulate PK/PD time profiles after different dosing regimens to help guide the dose selection in future clinical studies.

KEY WORDS: monoclonal antibody; pharmacokinetics/pharmacodynamics; mechanism-based model; human; T cells; tolerance.

INTRODUCTION

$CD4^+$ T cells are key mediators in the initiation and perpetuation of both normal and pathogenic immune responses directed against self-antigens, which can contribute to autoimmune diseases and organ rejection in transplantation. Anti-CD4 antibodies have been consistently shown to induce durable, antigen-specific tolerance to soluble proteins (1,2) and tissue organ transplants (3,4), and to reestablish self-tolerance in rodent model of autoimmune disease (5,6). However, successfully transferring these positive results from rodent models into the clinical setting has met with disappointing results. Over the past several years, several different anti-CD antibodies have been evaluated in clinical studies encompassing a wide range of indication including rheumatoid arthritis (7–9), multiple sclerosis (10–12), psoriasis (13,14), transplant, Crohn's disease (15,16), and asthma (17). However, the therapeutic effectiveness of these antibodies was modest at best, of short duration, and most likely the consequence of transient immunosuppression. Failure of these anti-CD4 antibodies to produce durable and robust response may be attributed to factors relating to both antibody properties and dose. For example, early clinical studies used murine and chimeric anti-CD4 antibodies that were highly immunogenic, and therefore elicited neutralizing human antimouse antibody and antichimeric antibody response that led to the rapid clearance of these anti-CD4 antibodies (10,17,18). Furthermore, many anti-CD4 antibodies used in previous clinical studies depleted $CD4^+$ T cells, and failed to recognize the advantages of nondepleting anti-CD4 antibodies because the major regulatory T-cell population mediated tolerance is CD4 itself (19,20). In addition, the dose of anti-CD4 antibodies used in most clinical studies, although sufficient to induce varying degrees of immunosuppression, may be too low to induce long-term immunological tolerance because of adverse side effects or the T-cell-depleting nature of these antibodies.

To overcome these potential limitations, a novel humanized anti-CD4 monoclonal IgG1κ antibody was developed to reduce immunogenicity. In addition, one of the amino acid in the Fc region of the heavy chain was modified to reduce FcR interactions and complement binding in order to avert CD4 depletion and infusion reactions. In nonhuman primates, it was demonstrated that a short course of high-dose TRX1 induced a long-term, antigen-specific tolerance to foreign

[1] Department of Pharmacokinetic and Pharmacodynamic Sciences, MS 70, Genentech Inc., 1 DNA Way, South San Francisco, California 94080, USA.
[2] TolerRx Inc., Cambridge, MA, USA.
[3] To whom correspondence should be addressed. (e-mail: Ng.chee@gene.com).

antigens without compromising normal immune function or depleting CD4 lymphocytes (21).

In this report we describe the pharmacokinetic (PK) and pharmacodynamic (PD) profiles of the anti-CD4 antibody TRX1 in normal human volunteers and show that anti-CD4 antibody TRX1 clearance is likely mediated in part by cellular binding and internalization. Furthermore, PK/PD data from the phase I study was used to develop a mechanism-based PK/PD model to describe the receptor-mediated drug disposition of TRX1 and its modulatory effect on CD4 receptors. This model was also utilized to simulate the PK/PD time profiles following different dosing regimens to help guide dose selection for future clinical studies.

MATERIALS AND METHODS

Antibody

TRX1 is a humanized monoclonal antibody with a molecular weight of 150 kDa, and composed of two identical heavy chains (composed of 44 amino acids each) and two identical light chains (composed of 218 amino acids each), each held together by disulfide bonds. The antibody was formulated for an intravenous infusion at 5.49 mg mL^{-1} in 20 mM histidine and was supplied in 5-mL glass vials with silicone polymerized butyl rubber stoppers and aluminum crimp seals.

Clinical Study Design

The phase I study was a single-center, double-blind, randomized, placebo-controlled study to investigate the safety, tolerability, PK, and PD of single rising doses of TRX1. The study was conducted at Quintiles Drug Metabolism and Pharmacokinetics Unit in Edinburgh, UK. Four healthy male subjects (per dose group) received a single 2-h intravenous infusion of TRX1 at the dose levels of 1, 5, and 10 mg kg^{-1}. Within each dose group, three subjects were randomized to receive TRX1 and one subject to receive placebo. The study was approved by the institutional review board; all subjects gave written informed consent for their participation in the study. A total of 12 subjects were enrolled in the study. Summary statistics of subject demographic details by treatment are shown in Table I. PK blood samples were collected at day 0 preinfusion, 0.5, 1, 2, 3, 5, 6, 8, 12, 24 h (day 1), 48 (day 2) and 72 h (day 3) after commencement of infusion, days 5, 7, 10, 15, 22, and 29, and every 2 weeks thereafter until CD4 levels returned to baseline. PD blood samples (5 mL) were collected from all the patients at the following times to measure total and free CD4 receptors: screening, day 1 (admission), day 0 preinfusion, 3, 12, 24 h (day 2), 48 h (day 3), and 72 h (day 3) after commencement of infusion, days 5, 7, 10, 15, 22, and 29, and thereafter every 2 weeks until TRX1 binding to lymphocytes was no longer detectable.

Analytical Methods

PK assay: Blood samples were drawn either by direct venipuncture or via an intravenous catheter and collected into plain vacutainers without anticoagulant. Samples were allowed to stand for 60 min to allow the clot to retract, and then centrifuged at 2500 rpm for 10 min at room temperature. The resulting serum was stored at −70°C until further analysis. Serum levels of TRX1 were determined using an enzyme-linked immunosorbent assay (ELISA). The assay was validated over the concentration range of 156–10,000 ng mL^{-1} TRX1 with precision ranging from 5.98 to 24.2%.

PD assay: Blood samples were collected into sodium heparin vacutainers and stored at ambient temperatures of 18–22°C. The samples were analyzed by flow cytometry using FACS-Calibur 4-color Analyzer (Becton Dickinson, Cowley, UK). One hundred microliters of blood was added to a tube (12 × 75 mm) containing 1 μg per stain of primary antibodies, i.e., CD8-FITC, CD4-PE, CD3-PerCP, CD45RA. Contents in the tube were mixed well and incubated in the dark at room temperature for 20 min, after which 2 mL of lysis reagent was added. Each tube was vortexed and incubated in the dark at room temperature for 10 min. The tubes were centrifuged for 5 min at 200 × *g* and the supernatant removed. The cells were then fixed by adding 0.5 mL of 1% paraformaldehyde and the tubes were stored until analysis (2–4 h) at 4°C.

The saturation of $CD4^+$ lymphocytes and monocytes was monitored by staining blood samples with TRX-1 biotin followed by fluorescein isothiocyanate (FITC)–streptavidin to detect free CD4 sites on cells. T lymphocytes and monocytes were identified by staining with CD3 and CD14, respectively. Coating of CD4 by TRX1 was detected in a separate tube by staining with F(ab′)2 fragment of goat antihuman IgG–biotin, followed by FITC–streptavidin. Data were reported as percent TRX1–biotin stained CD3(+) and

Table I. Summary of Subject Demographic Characteristics

	TRX1			
Parameters	1 mg kg^{-1} (n = 3)	5 mg kg^{-1} (n = 3)	10 mg kg^{-1} (n = 3)	Placebo (n = 3)
Age (years)	27.0 (27–27)	25.7 (23–30)	41.7 (39–43)	30.0 (23–37)
Weight (kg)	80.0 (67 –99)	79.9 (76–87)	90.8 (84–99)	85.7 (85–87)
BMI (kg m^{-2})	23.3 (22–26)	24.3 (23–26)	28.3 (26–30)	25.7 (25–26)
Race				
White	1	3	2	3
Africa America	1	0	0	0
Others	1	0	1	0

Values indicate mean (range).

CD14(+) cells and percent antihuman IgG stained CD3(+) and CD14(+) cells. Mean channel fluorescence (MCF) was reported for each population as well.

Isolation of Human T Cells

Human T cells were isolated from 100 mL of anonymous whole donor blood using T-cell Negative Isolation Kit (22) (Dynal Biotech, Lake Success, NY, USA). Lymphocytes were separated from whole blood using the Ficoll gradient method (ICN Pharmaceuticals Biochemicals Division, Aurora, OH, USA). The isolated lymphocytes were then suspended in 20 mL of complete media (RPMI 1640, 10% fetal bovine serum, 1% glutamine, 1% penicillin/streptomycin, and 1% sodium pyruvate) in a tissue culture flask and placed in a humidified 37°C tissue incubator for 1 h to allow monocytes and macrophages to attach. Following incubation, the unattached cells were removed from the flasks and resuspended at 10^7 cells per 200 µl of PBS containing 0.1% bovine serum albumin. Twenty microliters of fetal bovine serum per 10^7 cells was added, followed by the addition of 20 µl of Antibody Mix (Dynal Biotech) for 10 min at 4°C. Excess antibody was washed out, and T cells were negatively separated followed by exposure to a magnetic source. Recovered T cells were greater than 97% in purity, as determined by flow cytometry using FITC-conjugated anti-CD3 monoclonal antibody (data not shown).

Wide-Field Fluorescent Microscopy

Human T cells were incubated with TRX1-488 at a ratio of 10^6 cells per 1 µg of antibody in 200 µl of PBS for 30 min at 4°C. The cells were washed and then incubated in the same volume with 1 µg of antihuman IgG for an additional 30 min at 4°C. Cells were then washed and incubated at 37°C for a range of time points. At the conclusion of each incubation time point, cells were placed on ice. At the conclusion of all time points, cells were incubated with 5 µM DiI for 5 min at 37°C or 50 nM LysoTracker Red for 30 min at 37°C to label the lysosomes (Molecular Probe, Eugene, OR, USA). In addition, cells were incubated for 5 min with 100 nM Hoechst 33342 (Calbiochem, Bad Soden, Germany) at 37°C to label the nucleus. Labeled cells were then attached to poly[L] lysine-coated plates and assessed for TRX1-488 antibody internalization and subcellular localization using wide-field fluorescent microscopy (22).

Data Analysis

Pharmacokinetic Variables

PK parameters of TRX1 were initially estimated by noncompartmental methods using WinNonlin Pro software, Version 3.1 (Pharsight Corporation, Mountain View, CA, USA). Maximum concentration (C_{max}) and time to C_{max} (T_{max}) were the observed values. Area under the plasma concentration–time curve from zero to last observable time (AUC_{last}) was estimated using the trapezoidal rule. Terminal half-life ($t_{1/2}$) was calculated using the terminal linear portion of the log concentration–time curve.

Pharmacodynamic Variables

The pharmacodynamic parameters, free CD4, and total CD4 sites were calculated for each subject at each time point. The PD parameters are represented as a ratio from baseline (using the average of PD estimates at screening, day −1, and day 0 preinfusion).

PK/PD Model

A receptor-mediated pharmacokinetic (PK)/pharmacodynamic (PD) model (23,24) characterizing the relationship between serum TRX1 concentration and total and free CD4 expression was developed (Fig. 1) and simultaneously fitted to both sets of PK/PD data. Drug in the plasma or central compartment was assumed to be eliminated by both nonspecific elimination (K_{el}) and specific receptor-mediated endocytosis. Receptor-mediated endocytosis was modeled as an interaction with free CD4 receptor (R_f) to form a drug-receptor complex (X_R) via reversible (K_{on} and K_{off}) binding, followed by cellular internalization (K_{int}). A tissue compartment with linear first-order distribution processes (K_{ct} and K_{tc}) was used to account for nonspecific drug binding or distribution.

The differential equations used to describe the PK/PD model (Fig. 1) of TRX1 are as follows:

$$\frac{dX_c}{dt} = R_0 - (K_{el} + K_{ct})X_c + K_{tc}X_t - \left(K_{on}\frac{X_c}{V_c}R_f - K_{off}X_R\right)V_c \quad (1)$$

$$\frac{dX_t}{dt} = K_{ct}X_c - K_{tc}X_t \quad (2)$$

$$\frac{dR_f}{dt} = K_{syn} - K_{deg}R_f - K_{on}\frac{X_c}{V_c}R_f + K_{off}X_R \quad (3)$$

$$\frac{dX_R}{dt} = K_{on}\frac{X_c}{V_c}R_f - K_{off}X_R - K_{int}X_R \quad (4)$$

where X_c and X_t are the amount of free TRX1 in central and tissue compartment, respectively; R_f and X_R are the free CD4 and TRX1–CD4 complex concentrations, respectively; K_{tc} and K_{ct} are the first-order distribution rate constants; K_{el} is the first-order nonspecific elimination rate constant from the

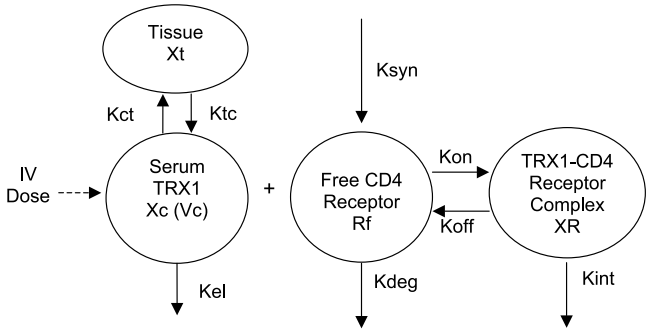

Fig. 1. Schematic representation of mechanism-based PK/PD model of TRX1.

central compartment; V_c is the volume of distribution of TRX1 in the central compartment; K_{syn} and K_{deg} are the zero-order synthesis rate and first-order elimination rate constants of free CD4 receptor, respectively; K_{on} and K_{off} are the association and dissociation rate constants for TRX1–CD4 binding, respectively; and K_{int} is the first-order internalization/degradation rate constant of CD4 receptor complex. SCL is the conversion factor to convert the fluorescent intensity value of free and total CD4 to concentration (nM).

This model was simultaneously fitted to the individual TRX1 concentration data, the total CD4 expression, and the free CD4 receptor sites by use of an iterative two-stage modeling approach (25) implemented in S-ADAPT II program, an augmented version of ADAPT II with population analysis capabilities (26,27). The intersubject variability was assumed to be log normally distributed and was fitted by use of an exponential model. A proportional error model was used to describe the intrasubject variability. With the assumption that the PK/PD system will remain constant after continuous exposure, the final model was then used to simulate the PK/PD profiles of the different multiple dosing regimens. The dose levels of TRX1 simulated were 1, 2, 3, 4, and 5 mg kg^{-1} i.v. infusion over 2 h on days 0, 4, 9, and 13.

RESULTS

In the study, TRX1 seemed to be well tolerated by the subjects, and first dose side effects, such as fevers, chills, and hypotension, were not observed. The 10 mg kg^{-1} dose group of TRX1 was associated with pruritic rashes in two out of three subjects. Both subjects were prescribed oral antihistamine. In both cases, the rashes were resolved completely. TRX1 did not deplete the total lymphocyte counts (Fig. 2). The pharmacokinetic parameters of TRX1 profiles (Fig. 3A–C), estimated using noncompartmental analyses, are shown in Table II. Serum TRX1 concentrations declined with a mean apparent terminal half-life of approximately 0.77 to 2.55 days over the dose range of 1–10 mg kg^{-1}. Following a single intravenous infusion of TRX1 administered over 2 h to healthy young subjects, C_{max} increased in a dose-proportional manner.

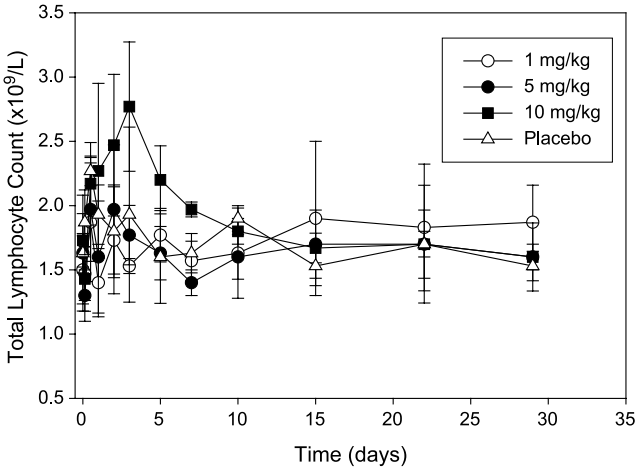

Fig. 2. Total lymphocyte counts–time profiles.

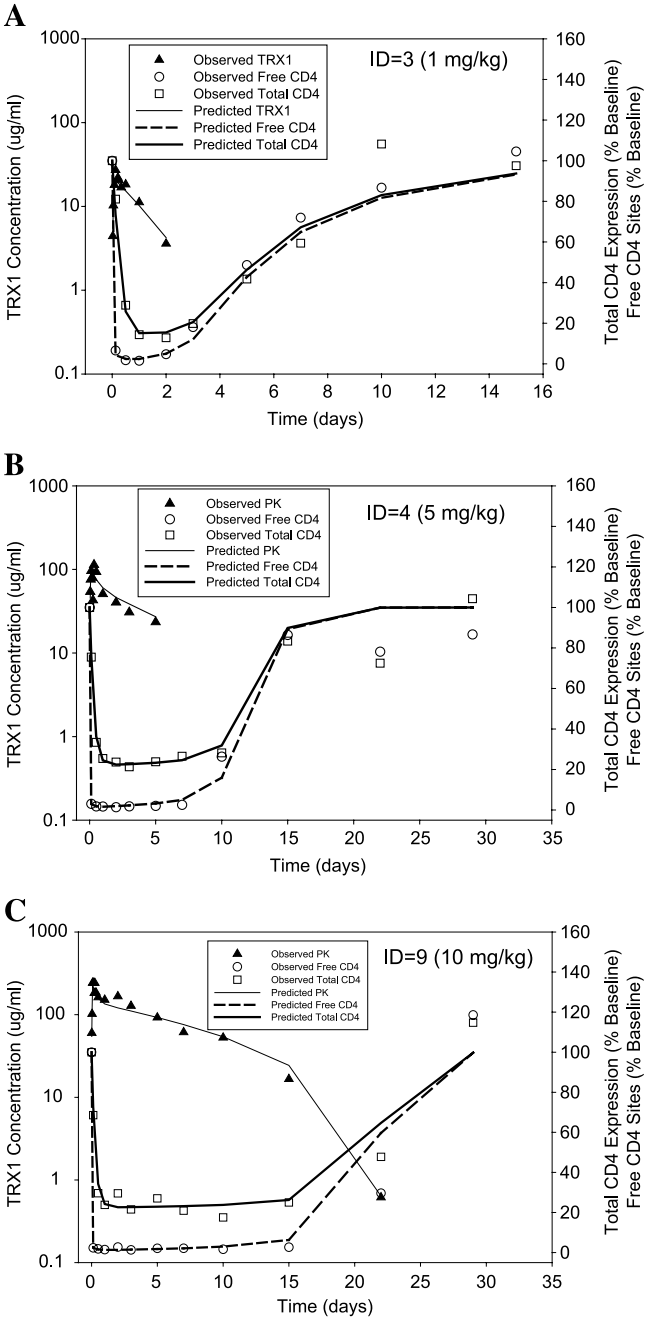

Fig. 3. Model fit of representative PK/PD profiles: (A) 1 mg kg^{-1}, (B) 5 mg kg^{-1}, (C) 10 mg kg^{-1}.

However, the extent of systemic exposure, $AUC_{0-\infty}$, increased in a greater than dose-proportional manner for TRX1 (i.e., dose-dependent kinetics) over the dose range 1–10 mg kg^{-1}, suggesting the nonlinearity of TRX1 pharmacokinetics. Serum TRX1 concentrations were below the limit of quantification of the assay in the three subjects following 1, 5, and 10 mg kg^{-1} TRX1 by days 5, 15, and 29, respectively.

The CD4 receptor levels were saturated by more than 90% relative to placebo and the duration of maximal effect lasted from 3 h post-TRX1 administration up to 3, 10, and 15 days, following the administration of 1, 5, and 10 mg kg^{-1} TRX1, respectively (Fig. 3A–C). The levels of total CD4

Table II. Noncompartmental Pharmacokinetic Parameters of TRX1 Administered as Single Intravenous Infusions at Dose Levels of 1, 5, and 10 mg kg^{-1}

Parameters	Group 1 (1 mg kg^{-1})	Group 2 (5 mg kg^{-1})	Group 3 (10 mg kg^{-1})
C_{max} (μg mL^{-1})	22.8 ± 3.9	104.7 ± 8.5	228.5 ± 17.4
$AUC_{0-\infty}$ (μg day mL^{-1})	26.8 ± 1.7	449.8 ± 155.7	1285.3 ± 105.9
CL (mL day^{-1} kg^{-1})	37.4 ± 2.4	12.0 ± 3.7	7.8 ± 0.6
Terminal $t_{1/2}$ (day)	0.77 ± 0.14	2.55 ± 0.89	2.00 ± 0.20

Mean ± SD (n = 3).

were reduced by more than 70% relative to placebo, and the duration of maximal effect and the start of the return to baseline levels at each dose level for total CD4 were similar to that of free CD4, with the exception of onset of maximal effect being 12 h post-TRX1 administration. Furthermore, the duration of maximum coating and down-modulation of CD4 receptors increased with increasing dose (Fig. 3A–C).

Wide-field fluorescent microscopy was used to assess the TRX1-induced internalization of CD4 and subcellular localization of T cell internalized TRX1 antibody in isolated human T cells. At time 0, TRX1-488 was localized to the plasma membrane (left panel, Fig. 4A). The internalization of TRX1-488 was observed as early as 15 min, and at 30 min, most of the TRX1-488 located on the plasma membrane was internalized, as there was noticeably less antibody associated with the plasma membrane relative to time 0. Aliquots of these cells incubated in the presence of TRX1-488 for 30 min at 37°C were labeled with LysoTracker Red and Hoechst 33342 to determine whether the internalized antibody is located within the lysosome. Results from this analysis are presented in Fig. 4B. The left panel represents the internalization of TRX1-488 by purified human T cells. The center panel shows the subcellular location of lysosomes in these cells, whereas the right panel shows the merged image of left and center panels, suggesting that the internalized TRX1-488 is located within the lysosomes.

A fully integrated mechanism-based PK/PD model was developed to describe the serum TRX1 and free and total CD 4 receptor time profiles in human subjects (Fig. 1). The nonlinear pharmacokinetic behavior of TRX1 was assumed to be primarily due to binding of the drug to the CD4 receptors. Figure 3A–C represents the model fitted TRX1 serum concentration, free CD4 sites, and the total CD4 expression data from phase I for subjects 3, 4, and 9, respectively. As shown in Fig. 3A–C, the model fitted the data reasonably well and helped explain the receptor-

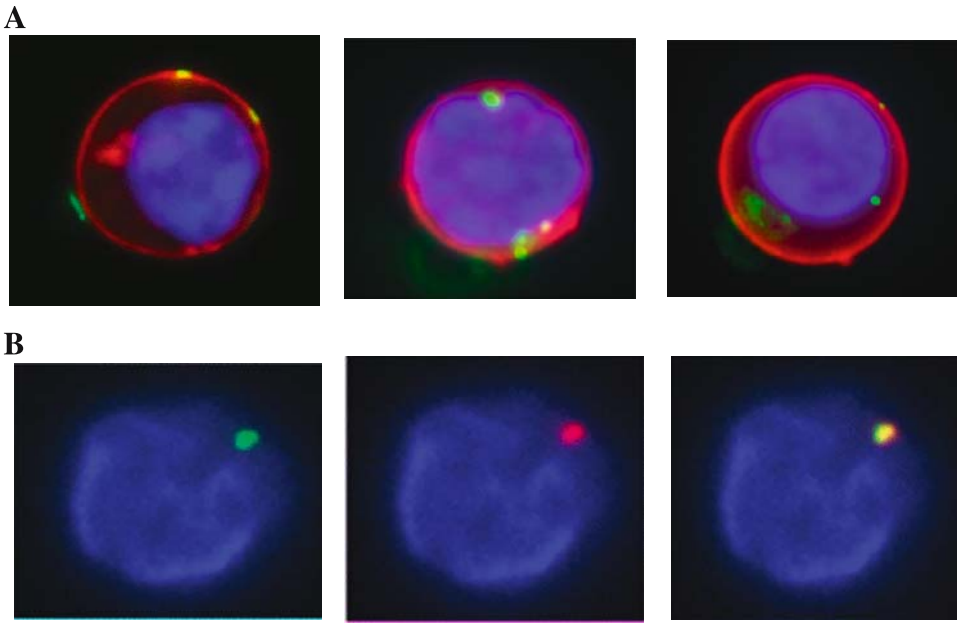

Fig. 4. Internalization and subcellular localization of TRX1. Wide-field fluorescent microscopy of purified human T cells incubated with TRX1 antibody conjugated to AlexaFluor 488 (green). (A) Cells were incubated with TRX1-488 and labeled with plasma membrane marker DiI (red) and cytoplasmic marker Hoechst 33342 (blue). The left, center, and right panels represent the internalization of TRX1-488 for 0, 15, and 30 min, respectively. (B) Cells were incubated with TRX1-488 for 30 min and then labeled with lysosome marker LysoTracker Red (red) and Hoechst 33342 (blue). The left panel shows the location of TRX1-488, the center panel shows the location of LysoTracker Red, and the right panel is the merged image of left and center panels.

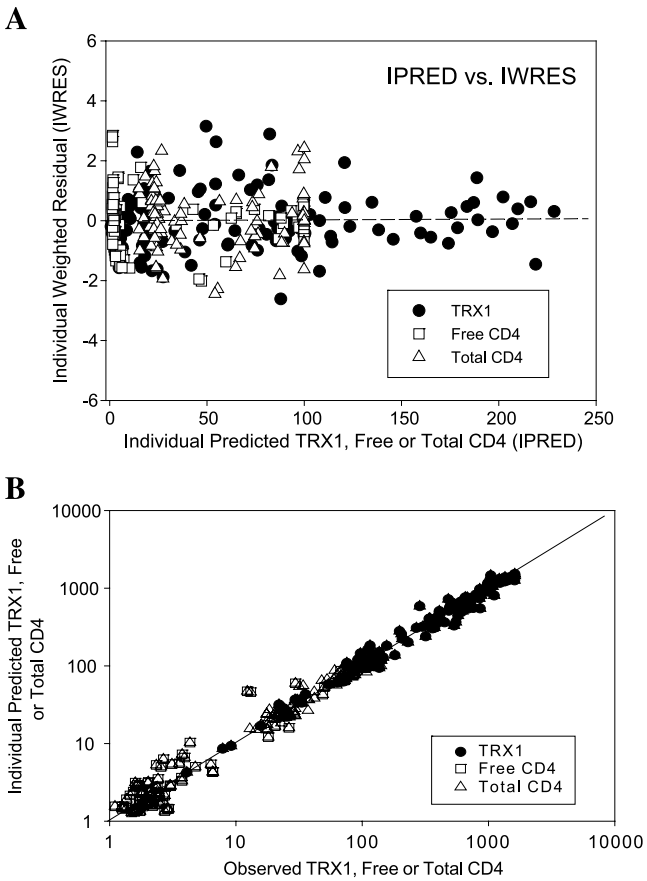

Fig. 5. Goodness-of-fit plot: (A) individual weighted residual *vs.* individual predicted TRX1, and free and total CD4 receptors; (B) individual observed *vs.* individual predicted TRX1, and free and total CD4 receptors.

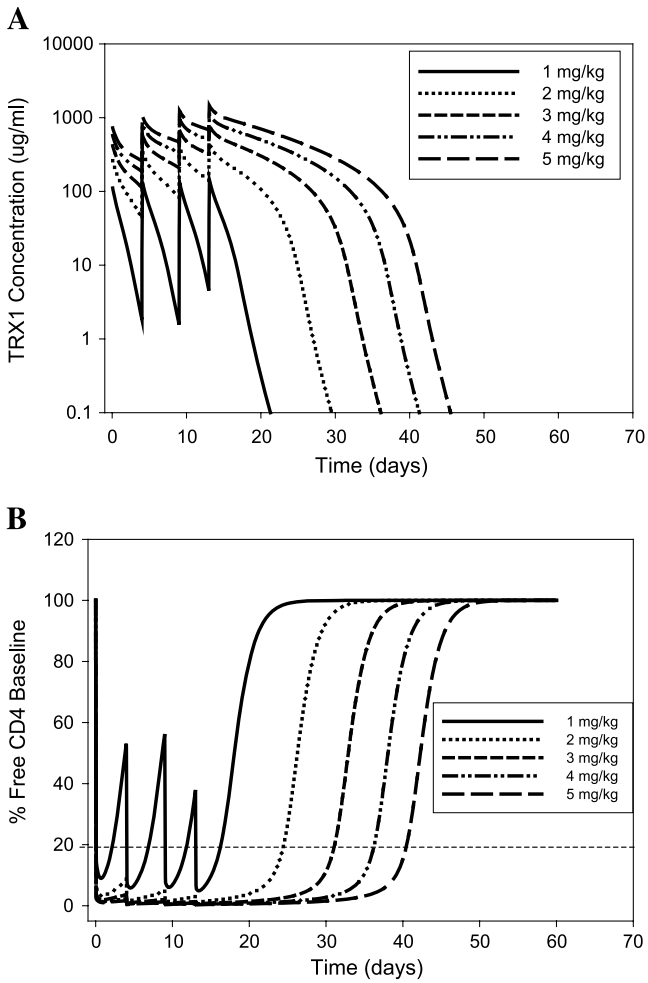

Fig. 6. Simulated (A) TRX-1 and (B) free CD4 receptor time profiles of different dosing regimens (1, 2, 3, 4, and 5 mg kg^{-1} i.v. infusion over 2 h on days 0, 4, 9, and 13).

mediated drug disposition for TRX1 and its effect on CD4 receptors in humans. The residuals were well distributed and there was no systematic bias identified in the goodness-of-fit plots (Fig. 5A and B). In addition, the % CV values calculated for the model parameter estimates were relatively low and indicative of a good model fit (Table III). The equilibrium dissociation constant K_d, calculated as the ratio of K_{off} and K_{on}, was estimated to be 19.38 nM, which indicates a high affinity of the antibody to the CD4 receptors.

The PK/PD model was utilized to simulate the data for a multiple dose regimen of TRX1 at various dose levels to help guide the dose selection process for future clinical studies. Simulated profiles were obtained for dosing regimens of 1, 2, 3, 4, and 5 mg kg^{-1} i.v. infused over 2 h on days 0, 4, 9, and 13 (Fig. 6). Figure 6A and B represents the simulated plasma concentration profiles for TRX1 and free CD4 receptor sites, respectively, at different dosing regimens. Based on the analysis of preclinical efficacy model, it is assumed that the reduction in free CD4 receptor levels could be utilized as a possible marker to aid in dose selection for future clinical doses (21). The CD4 levels at the 1 mg kg^{-1} dose level recovered to greater than 50% of baseline before the second and third doses, and greater than 35% before the fourth dose (Fig. 6B). However, as evident in Fig. 6B, free CD4 receptors were persistently below set target of 20% up to 24, 31, 36, and 40 days at the 2, 3, 4, and 5 mg kg^{-1} level.

Figure 7 represents the percentage of contribution of receptor-mediated clearance of TRX1 at various dose levels. It is evident that at lower dose levels the clearance mechanism due to receptor-mediated endocytosis contributed more toward the elimination of the drug than at the higher dose levels because of the saturation of the receptor at higher doses. The contribution of the receptor-mediated clearance ranged from 58.5 to 94.4% at various dose levels.

Table III. PK/PD Parameters Estimates from the Model

Parameter	Model estimates (% CV)
K_{el} (day^{-1})	0.078 (21.4)
K_{ct} (day^{-1})	0.649 (15.9)
K_{tc} (day^{-1})	0.874 (24.9)
V_c (ml kg^{-1})	41.7 (3.3)
K_{deg} (day^{-1})	0.694 (5.5)
K_{on} (nM day^{-1})	0.753 (16.1)
K_{off} (day^{-1})	14.6 (18.5)
K_{int} (day^{-1})	3.93 (7.3)
SCL (nM $\%^{-1}$)	0.549 (6.7)

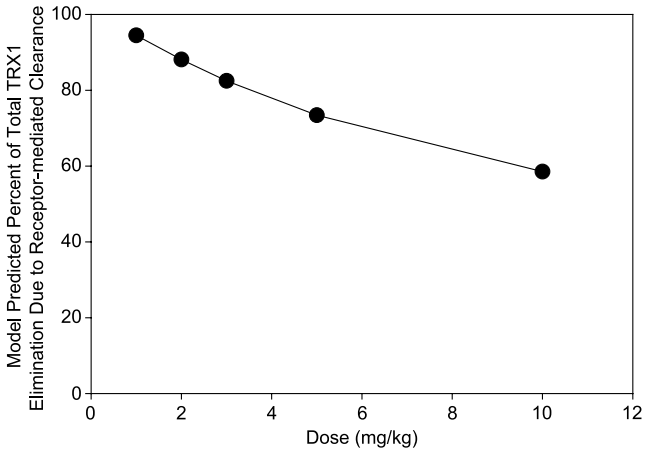

Fig. 7. Simulated percentage of total TRX1 elimination due to receptor-mediated clearance at various dose levels.

DISCUSSION

TRX1, an anti-CD4 monoclonal IgG1 antibody, is currently being developed to induce tolerance against foreign proteins, biologic therapeutics, allograft-transplanted organs, and ultimately to self-antigens in autoimmune settings by blocking CD4-mediated functions. In this first human trial of TRX1, pharmacokinetics and pharmacodynamics were investigated after a single intravenous infusion (1–10 mg kg^{-1}) in healthy normal volunteers. The convex shape of the serum concentration–time profiles, and greater than dose-proportional increase in systemic exposure ($AUC_{0-\infty}$) from a dose range 1–10 mg kg^{-1} suggested that TRX1 pharmacokinetics in humans is nonlinear. Although TRX1 does not affect the number of circulating T cells (Fig. 2), it does coat and down-modulate the CD4 receptors in a dose- and concentration-dependent manner. Coating and down-modulation of the CD4 antigen by TRX1 were evident in all dose groups studied. The duration of maximum coating and down-modulation of CD4 receptors increased with increasing dose from 1 to 10 mg kg^{-1}. Overall, the pharmacokinetic and pharmacodynamic profiles of TRX1 suggested that receptor-mediated clearance of TRX1 may represent one mechanism by which TRX1 is cleared, and CD4 receptor was saturated and down-modulated after TRX1 treatment in human subjects. In general, majority of the antibodies that modulate the cell surface antigen expression do so through a process similar to receptor-mediated endocytosis of the entire immunocomplex, where the antibody and antigen enter common or distinct pathways for recycling and/or degradation (28). A recent study using human T cells as a model to study the cellular uptake and clearance of efalizumab suggested that this anti-CD11a monoclonal IgG1 antibody is internalized by purified T cells. This CD11a-mediated internalization constitutes one important pathway by which efalizumab is cleared in human (22). Therefore, it is possible that the receptor-mediated clearance of TRX1 and CD4 receptor saturation and down-modulation observed in this study may be mediated by cellular internalization of the TRX1–CD4 receptor complex. Using the purified human T-cell model, we showed that TRX1 was internalized *in vitro* by human T cells. In addition, the internalized TRX1 was found in subcellular organelles that stained positive for LysoTracker, the fluorescent marker for lysosomes. These results suggested that CD4-mediated internalization and lysosomal targeting of TRX1 may be one pathway by which this antibody is cleared in human.

The findings from the *in vitro* study were then used to develop a mechanism-based PK/PD model that describes the PK/PD behavior of TRX1 after the i.v. infusion of various dose levels in human subjects. The proposed model described the relationship between serum TRX1 concentration and total and free CD4 reasonably well. The final estimated value of V_c (41.7 mL kg^{-1}) closely resembles the plasma volume in humans ($\sim$42.8 mL kg^{-1}) (29), as is expected for a high molecular weight protein and was consistent with the values reported for other monoclonal IgG1 antibodies (30,31). The elimination rate constant (K_{el}) is 0.078 $days^{-1}$, and represents the elimination of TRX1 from the central compartment in the absence of receptor-mediated endocytosis. Therefore, the theoretical β phase elimination half-life in the absence of receptor-mediated endocytosis can be calculated using the following equation:

$$t_{1/2\beta} = 2{*}0.693/\left[(K_{tc} + K_{ct} + K_{el}) - \sqrt{(K_{tc} + K_{ct} + K_{el})^2 - 4K_{tc}K_{el}}\right] = 15.9 \text{ days}$$

This value falls within the range of 15–21 days of the β phase half-life of natural IgG in human (32). The TRX1–CD4 dissociation rate constant, K_d, calculated as the ratio of the model estimated K_{off} and K_{on} values, is estimated as 19.38 nM. This finding is different than the K_d values of 0.6 ± 0.3 nM obtained from *in vitro* studies (unpublished data; TolerRx, Inc.). One possible reason for the difference is that the K_d value estimated from the model reflects the binding affinity in a "real-time" clinical setting (i.e., within an open and dynamic biological system with disposition pathways for free TRX1, free CD4, and TRX1–CD4 complexes), whereas the K_d values estimated by *in vitro* binding studies were performed under closed microsystem with controlled experimental conditions.

The model takes into account the receptor-mediated endocytosis and nonspecific mechanism of elimination as the elimination pathway of TRX1. Therefore, the total systemic clearance of the TRX1 (CL_{total}) can be calculated as follows (24):

$$CL_{total} = K_{el}V_c + (R_{total} - DR)V_c\left(\frac{K_{int}}{K_{int} + K_{off}}\right)$$

where R_{total} is the amount of total CD4 receptors. When the TRX1 concentration is very high, DR $\rightarrow R_{total}$ and CL_{total} was reduced to $K_{el}V_c$, which is a clearance due to nonspecific elimination pathways. Likewise, when the TRX1 concentrations is very low compared to amount of total CD4 receptors, DR $\rightarrow$ 0, and the CL_{total} becomes:

$$CL_{total} = K_{el}V_c + K_{on}R_{total}V_c\left(\frac{K_{int}}{K_{int} + K_{off}}\right)$$

Therefore, it is expected that at a very high TRX1 concentration in patients who receive large doses, the receptor-

mediated elimination of TRX1 will become less significant, and the elimination of TRX1 is mainly attributable to linear nonspecific elimination pathways. Therefore, the contribution of CD4 receptor-mediated pathways on TRX1 elimination should decrease as the dose increases. This was confirmed by comparing the values of $K_{el}V_c$ obtained from the model to the clearance obtained from the noncompartmental analysis of i.v. single-dose data. The contribution of the nonspecific mechanism of elimination, K_{el}, was thus calculated to be 8.6, 27.1, and 41.7% of the clearance values at 1, 5, and 10 mg kg^{-1} dose levels, respectively; this finding was further supported by using the simulation study. Figure 7 represents the simulated percentage of eliminated drug due to receptor-mediated clearance mechanisms after a single dose administration. The values obtained for the contribution of the nonspecific clearance of TRX1 are similar to the ones obtained as a ratio of $K_{el}V_c$ and total clearance. It is evident that K_{el} does not represent a significant mechanism of elimination until higher i.v. doses (5 mg kg^{-1}) are administered. This can be explained by the hypothesis that receptor-mediated elimination pathway is saturated at higher doses and the contribution of receptor-mediated endocytosis decreases as dose increases.

TRX1 is currently in development for induction of tolerance in autoimmune diseases and organ transplants. Results from the preclinical and phase I studies with TRX1 were promising and indicated that the free CD4 levels could be reduced below 20% baseline up to a period of 15 days at the highest dose level. To achieve reduction in free CD4 levels for an extended period of time, a regimen of multiple i.v. infusions could be further administered. However, the determination of the number and optimal schedule of infusions in human population is associated with a financial and time constraint. Therefore a PK/PD model explaining the disposition of drug in relation to the expression of free receptor sites would lend an understanding in the feasibility and design of a rational clinical study. In this study we have developed an integrated PK/PD model to characterize the i.v. dosing of TRX1 at various dose levels in humans. The developed model described the serum TRX1 and free and total CD4 receptor time profiles reasonably well. The developed PK/PD model was used to simulate PK/PD time profiles after different dosing regimens to guide dose selection in future clinical studies.

ACKNOWLEDGMENT

The authors would like to thank Benjamin Wu for his technical assistance.

REFERENCES

1. N. L. Gutstein, W. E. Seaman, J. H. Scott, and D. Wofsy. Induction of immune tolerance by administration of monoclonal antibody to L3T4. *J. Immunol.* **137**:1127–1132 (1986).
2. S. Qin, S. Cobbold, H. Tighe, R. Benjamin, and H. Waldmann. CD4 monoclonal antibody pairs for immunosuppression and tolerance induction. *Eur. J. Immunol.* **17**:1159–1165 (1987).
3. S. P. Cobbold, G. Martin, and H. Waldmann. The induction of skin graft tolerance in major histocompatibility complex-mismatched or primed recipients: primed T cells can be tolerized in the periphery with anti-CD4 and anti-CD8 antibodies. *Eur. J. Immunol.* **20**:2747–2755 (1990).
4. S. E. Marshall, S. P. Cobbold, J. D. Davies, G. M. Martin, J. M. Phillips, and H. Waldmann. Tolerance and suppression in a primed immune system. *Transplantation* **62**:1614–1621 (1996).
5. P. Hutchings, L. O'Reilly, N. M. Parish, H. Waldmann, and A. Cooke. The use of a non-depleting anti-CD4 monoclonal antibody to re-establish tolerance to beta cells in NOD mice. *Eur. J. Immunol.* **22**:1913–1918 (1992).
6. J. M. Phillips, S. Z. Harach, N. M. Parish, Z. Fehervari, K. Haskins, and A. Cooke. Nondepleting anti-CD4 has an immediate action on diabetogenic effector cells, halting their destruction of pancreatic beta cells. *J. Immunol.* **165**:1949–1955 (2000).
7. C. Herzog, C. Walker, W. Muller, P. Rieber, C. Reiter, G. Riethmuller, P. Wassmer, H. Stockinger, O. Madic, and W. J. Pichler. Anti-CD4 antibody treatment of patients with rheumatoid arthritis. I. Effect on clinical course and circulating T cells. *J. Autoimmun.* **2**:627–642 (1989).
8. G. Horneff, G. R. Burmester, F. Emmrich, and J. R. Kalden. Treatment of rheumatoid arthritis with an anti-CD4 monoclonal antibody. *Arthritis Rheum.* **34**:129–140 (1991).
9. G. Horneff, F. Emmrich, and G. R. Burmester. Advances in immunotherapy of rheumatoid arthritis: clinical and immunological findings following treatment with anti-CD4 antibodies. *Br. J. Rheumatol.* **32**(Suppl 4):39–47 (1993).
10. E. Racadot, L. Rumbach, M. Bataillard, J. Galmiche, J. L. Henlin, M. Truttmann, P. Herve, and J. Wijdenes. Treatment of multiple sclerosis with anti-CD4 monoclonal antibody. A preliminary report on B-F5 in 21 patients. *J. Autoimmun.* **6**:771–786 (1993).
11. B. W. van Oosten, M. Lai, F. Barkhof, D. H. Miller, I. F. Moseley, A. J. Thompson, S. Hodgkinson, and C. H. Polman. A phase II trial of anti-CD4 antibodies in the treatment of multiple sclerosis. *Mult. Scler.* **1**:339–342 (1996).
12. B. W. van Oosten, M. Lai, S. Hodgkinson, F. Barkhof, D. H. Miller, I. F. Moseley, A. J. Thompson, P. Rudge, A. McDougall, J. G. McLeod, H. J. Ader, and C. H. Polman. Treatment of multiple sclerosis with the monoclonal anti-CD4 antibody cM-T412: results of a randomized, double-blind, placebo-controlled, MR-monitored phase II trial. *Neurology* **49**:351–357 (1997).
13. A. B. Gottlieb, M. Lebwohl, S. Shirin, A. Sherr, P. Gilleaudeau, G. Singer, G. Solodkina, R. Grossman, E. Gisoldi, S. Phillips, H. M. Neisler, and J. G. Krueger. Anti-CD4 monoclonal antibody treatment of moderate to severe psoriasis vulgaris: results of a pilot, multicenter, multiple-dose, placebo-controlled study. *J. Am. Acad. Dermatol.* **43**:595–604 (2000).
14. P. Morel, J. P. Revillard, J. F. Nicolas, J. Wijdenes, H. Rizova, and J. Thivolet. Anti-CD4 monoclonal antibody therapy in severe psoriasis. *J. Autoimmun.* **5**:465–477 (1992).
15. V. Canva-Delcambre, S. Jacquot, E. Robinet, M. Lemann, C. Drouet, M. Labalette, J. P. Dessaint, D. Bengoufa, C. Rabian, R. Modigliani, J. Wijdenes, J. P. Revillard, and J. F. Colombel. Treatment of severe Crohn's disease with anti-CD4 monoclonal antibody. *Aliment. Pharmacol. Ther.* **10**:721–727 (1996).
16. A. Stronkhorst, S. Radema, S. L. Yong, H. Bijl, I. J. ten Berge, G. N. Tytgat, and S. J. van Deventer. CD4 antibody treatment in patients with active Crohn's disease: a phase 1 dose finding study. *Gut* **40**:320–327 (1997).
17. B. M. Meiser, C. Reiter, H. Reichenspurner, P. Uberfuhr, E. Kreuzer, E. P. Rieber, G. Riethmuller, and B. Reichart. Chimeric monoclonal CD4 antibody—a novel immunosuppressant for clinical heart transplantation. *Transplantation* **58**:419–423 (1994).
18. G. Horneff, T. Winkler, J. R. Kalden, F. Emmrich, and G. R. Burmester. Human anti-mouse antibody response induced by anti-CD4 monoclonal antibody therapy in patients with rheumatoid arthritis. *Clin. Immunol. Immunopathol.* **59**:89–103 (1991).
19. S. X. Qin, M. Wise, S. P. Cobbold, L. Leong, Y. C. Kong, J. R. Parnes, and H. Waldmann. Induction of tolerance in peripheral T cells with monoclonal antibodies. *Eur. J. Immunol.* **20**:2737–2745 (1990).

20. S. X. Qin, S. Cobbold, R. Benjamin, and H. Waldmann. Induction of classical transplantation tolerance in the adult. *J. Exp. Med.* **169**:779–794 (1989).
21. D. Winsor-Hines, C. Merrill, M. O'Mahony, P. E. Rao, S. P. Cobbold, H. Waldmann, D. J. Ringler, and P. D. Ponath. Induction of immunological tolerance/hyporesponsiveness in baboons with a nondepleting CD4 antibody. *J. Immunol.* **173**:4715–4723 (2004).
22. G. P. Coffey, E. Stefanich, S. Palmieri, R. Eckert, J. Padilla-Eagar, P. J. Fielder, and S. Pippig. *In vitro* internalization, intracellular transport, and clearance of an anti-CD11a antibody (Raptiva) by human T-cells. *J. Pharmacol. Exp. Ther.* **310**:896–904 (2004).
23. G. Levy. Pharmacologic target-mediated drug disposition. *Clin. Pharmacol. Ther.* **56**:248–252 (1994).
24. D. E. Mager and W. J. Jusko. General pharmacokinetic model for drugs exhibiting target-mediated drug disposition. *J. Pharmacokinet. Pharmacodyn.* **8**:507–532 (2001).
25. J. L. Steimer, A. Mallet, J. L. Golmard, and J. F. Boisvieux. Alternative approaches to estimation of population pharmacokinetic parameters: comparison with the nonlinear mixed-effect model. *Drug Metab. Rev.* **15**:265–292 (1984).
26. D. D'Argenio and A. Schumitzky. ADAPT II user's guide: pharmacokinetic/pharmacodynamic system analysis software, Biomedical Simulations Resources, Los Angeles, 1997.
27. R. J. Bauer and S. Guzy. Monte Carlo Parametric Expectation Maximization (MC-PEM) method for analyzing population pharmacokinetic/pharmacodynamic (PK/PD) data. In D. Z. D'Argenio (ed.), *Advanced Methods of Pharmacokinetic and Pharmacodynamic System Analysis*, Vol. 3., Kluwer Academic Publishers, Boston, 2004, pp. 135–163.
28. T. Wileman, C. Harding, and P. Stahl. Receptor-mediated endocytosis. *Biochem. J.* **232**:1–14 (1985).
29. B. Davies and T. Morris. Physiological parameters in laboratory animals and humans. *Pharm. Res.* **10**:1093–1095 (1993).
30. J. Lu, J. Gaudreault, W. F. Novotny, B. Lum, and R. Bruno. A population pharmacokinetic model for Bevacizumab. *Clin. Pharmacol. Ther.* **75**:91 (2004).
31. K. A. Harris, C. B. Washington, G. Lieberman, J. Lu, R. Mass, and R. Bruno. A population pharmacokinetic (PK) model for trastuzumab (Herceptin) and implications for clinical dosing. *Proc. Am. Soc. Clin. Oncol.* **21**:488a (2002).
32. T. A. Waldmann and W. Strober. Metabolism of immunoglobulins. *Prog. Allergy* **13**:1–110 (1969).